

# Exploring the Spatio-Temporal Patterns of Normalised Difference Vegetation Index (NDVI) in Varanasi: An Analysis of Vegetation Dynamics

NazreenKhanam<sup>1\*</sup>, Lubna Siddiqui<sup>2\*\*</sup>, Neha Parveen<sup>3\*</sup>, Md NawajSarif<sup>4\*</sup>, Md Safikul Islam<sup>5\*\*\*</sup>,  
Shahanshah Khan<sup>6\*</sup>, Sheikh Mohibul<sup>7\*</sup>

\*Research Scholar, Department of Geography, Jamia Millia Islamia, New Delhi, India

\*\*Professor, Department of Geography, Jamia Millia Islamia, New Delhi, India

\*\*\*Post-Doctoral Fellow, Dr. Ambedkar International Centre (DAIC) and Department of Geography, Jamia Millia Islamia, New Delhi, India

**Corresponding Author:** Dr. Lubna Siddiqui<sup>2</sup>,

Room No. 114, Department of Geography, JamiaMilliaIslamia,  
New Delhi-110025

**Abstract:-** This study uses the Normalised Difference Vegetation Index (NDVI) from 1992 to 2019 to examine the spatiotemporal patterns of vegetation dynamics in Varanasi, India. A popular remote sensing index for observing vegetation dynamics is NDVI. Landsat photos and Geographic Information System (GIS) software are used to conduct the analysis. The findings show that there are considerable differences in NDVI values between various land cover types and seasons. According to the study, Varanasi's vegetation cover has fluctuated over the last three decades, with an overall trend in recent years towards lower NDVI values. In particular, the minimum NDVI ranged from -0.0858 (1992) to -0.0518 (2019) while the maximum NDVI ranged from 0.5799 (1992) to 0.4862 (2019) throughout the pre-monsoon season. The results of this study offer relevant information about the spatiotemporal patterns of vegetation dynamics in Varanasi and can guide policy choices for urban planning and sustainable land use.

**Keywords:-** Normalized Difference Vegetation Index, NDVI, Spatio-Temporal Analysis, Vegetation Dynamics, Varanasi, Remote Sensing, GIS, Time Series Analysis.

## I. INTRODUCTION

The Normalized Difference Vegetation Index (NDVI) is widely recognized as a crucial remote sensing analytical tool for simplifying multi-spectral imagery complexities. It has gained immense popularity and extensive usage in vegetation assessment. This widespread adoption is primarily attributed to the versatility of calculating NDVI using any multispectral sensor equipped with a visible and a near-infrared band. Multispectral sensors' decreasing costs and weights have enabled their deployment on various platforms, including satellites, aerial vehicles, and Unmanned Aerial Systems (UAS).

The Earth's vegetation cover is crucial to understanding the role of vegetation in global ecosystems and how land-atmosphere interactions affect climate. Changes in plant transpiration, surface albedo, emissivity, and roughness have a direct impact on surface water and energy budgets. (Ramankutty & Foley, 1999).The fractional

area of the vegetation that occupies each grid cell (horizontal density) and the leaf area index (LAI), or the number of leaf layers of the vegetated region (vertical density), are typically used to parameterize the amount of vegetation.)(Gutman, 1998).A popular vegetation measure that improves information about vegetation is the Normalised Difference Vegetation measure (NDVI). The red and infrared bands of the Landsat data were used to determine the NDVI using the equation (Eq. 4) suggested by Gao (1996). This is because the electromagnetic spectrum's NIR and red portions are where chlorophyll absorbs the greatest energy, making these ratios appropriate for NDVI computations. (Falguni Mukherjee, 2022; Shahfahad et al., 2020).

The link between NDVI and vegetation fraction as well as the extraction of the green vegetation fraction from NDVI have both been the subject of extensive investigation. However, difficulties and uncertainties arise by the fact that one NDVI measurement does not allow the simultaneous derivation of green vegetation fraction and local LAI. Gutman and Ignatov (1998) resolved this problem by prescribing local LAI equal to infinity and derived green vegetation cover from a scaled NDVI taken between bare soil NDVI and dense vegetation NDVI(Glenn, 2007; Gutman, 1998). Wittich and Hansing (1995) investigated the relationship between NDVI and vegetation fraction at five test sites in Germany and demonstrated that, roughly speaking, the linear expression of NDVI over a wide distribution of heterogeneous vegetation densities was sufficient to describe the vegetation cover fraction (Weng, 2009; Wittich, 1995). Several other studies also showed a strong linear relation between fractional vegetation cover and NDVI (Kustas, 2003; Ormsby, 1982; Wittich, 1995).However, several studies discovered a nonlinear link between NDVI and vegetation percentage, with NDVI producing unique curves with changes in plant cover correlating to various soil types (Glenn, 2007; Huete, 1985).

Few studies have looked at the relationship between NDVI and fractional vegetation while taking the scale effect of NDVI into consideration. The objective of this paper is to Explore the Spatio-Temporal Patterns of Normalised

Difference Vegetation Index (NDVI) in Varanasi from 1992-2019.

Multi-spectral photography is used in remote sensing to produce composite images for interpretation and analysis. To facilitate study, specific traits and patterns can be highlighted by transforming specific composite bands. These band changes, which are now widely used for information extraction, can create improved representations of ground objects like plants. Over one hundred vegetation indices have been derived from multispectral imagery, including the widely used Normalized Difference Vegetation Index (NDVI) proposed by Kriegl et al. (1969)(Karthi, 2022). The NDVI is popular due to its simplicity and ability to quickly delineate vegetation and vegetative stress, making it useful in commercial agriculture and land-use studies.

## II. STUDY AREA

One of the oldest populous towns in the world is Varanasi (also known as Kashi or Banaras). The city is situated in the eastern section of Uttar Pradesh, in the middle of the Ganges Valley in North India, through the crescent-shaped Ganges bank on the left, at a height of 15 to 21 metres (50 to 70 feet) on average. The district headquarters of its region is also Varanasi City. The city's urban

agglomeration area stretches from  $82^{\circ} 56'E$  to  $83^{\circ} 03'E$  and  $25^{\circ} 14'N$  to  $25^{\circ} 23.5'N$  (Fig. 1.). Varanasi had registered a population of about 1.2million (Census of India, 2011). and covered an area of  $82 \text{ km}^2$ , it is a smaller city with the potential to transcend conventional development approaches and has a faster urban growth than other cities. The city is divided into 90 wards for administrative purposes (Verma et al., 2020). A study was performed at the city level to provide a holistic understanding of the heterogeneity of Remote sensing spectral indices at a micro-scale level by using the ward boundary which can be applied at a wider scale for other similar cities.

Temperature typically varies between  $22^{\circ}\text{C}$  and  $46^{\circ}\text{C}$  (Karthi, 2022; Singh et al., 2019). The location map of the study area is shown in Figure 1. The city normally experiences a humid subtropical climate with four distinct seasons: monsoon (JAS), pre-monsoon (MAMJ), cold and moist winter (DJ), and post-monsoon (ON). The city periodically endures unusually dry, hot summer heat waves throughout the summer (called locally as Loo) and frigid winter spells. The summertime maximum temperature can reach  $46^{\circ}\text{C}$ , while the wintertime minimum temperature is typically about  $2^{\circ}\text{C}$ . (Murari et al., 2017; Nidhi Singh et al., 2019).

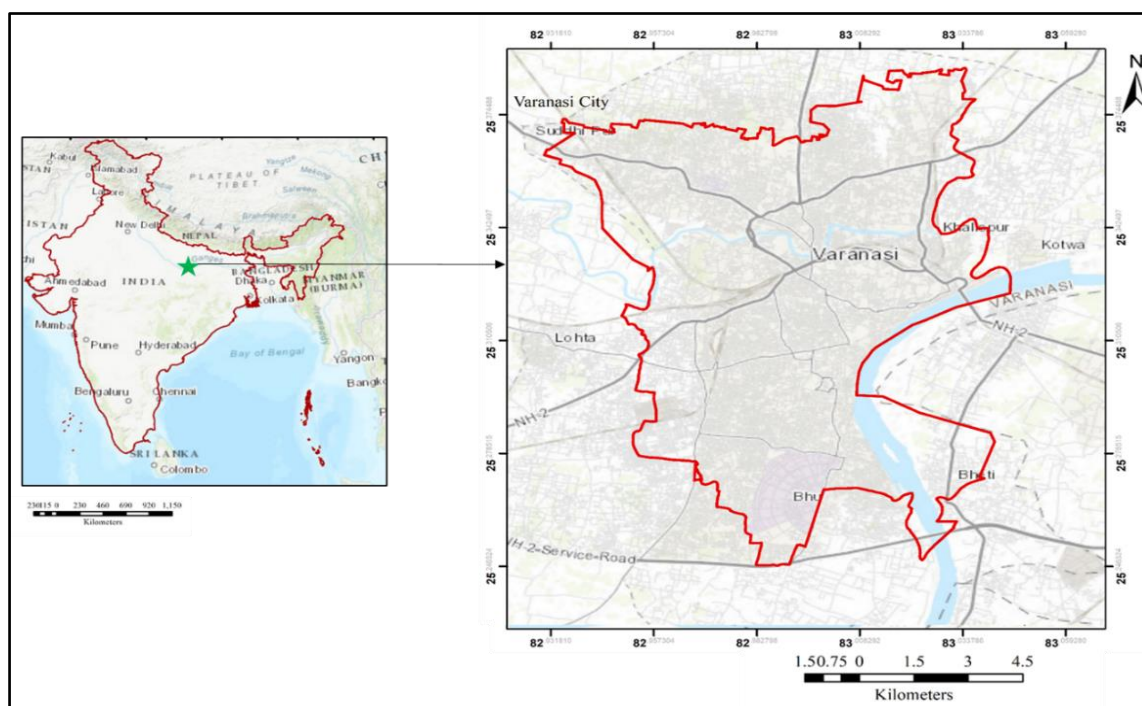


Fig. 1: Location Map of Varanasi City, India

## III. MATERIALS AND METHODOLOGY

Landsat satellite images were obtained from the USGS Earth Explorer website (<https://earthexplorer.usgs.gov/>) (Babita Kumari et al., 2018a). Before processing, the satellite data has previously undergone geometric adjustment and radiometric correction. Multi-temporal Landsat 5 TM and Landsat 8 OLI/TIRS data projected to WGS -1984 and UTM zone 45 o North for the

years 1992 and 2019 were the data used for the study (Table 1). (Arnous, 2022; Avdan & Jovanovska, 2016; Cruz et al., 2020; Mukherjee, 2022). Additionally, the Survey of India (SOI) Toposheet at a scale of 1: 20,000 was used to extract an area of interest (AOI) using the ERDAS Imagine version 9.3 software. ArcGIS 10.8 software was used to calculate Normalised differential vegetation index (NDVI) (Babita Kumari et al., 2018b).

Table 1: Satellite Data Meta Data and Band Values Used for LST and Spectral Indices calculation.

Sensor	Acquisition Year	AcquisitionDate/ Month	Band	Band Range	Resolution (Meter)
Landsat 5 TM	1992	04-03-2022	B1= BLUE	0.45-0.52	30*30
		28-09-1992	B2=GREEN	0.52-0.60	30*30
			B3=RED	0.63-0.69	30*30
			B4=NIR	0.76-0.90	30*30
			B6=TIR	10.40-12.50	Resample
Landsat 8 OLI	2019	31-03-2019	B2=BLUE	0.452-0.512	30*30
		10-11-2019	B3=GREEN	0.533-0.590	30*30
			B4=RED	0.636-0.673	Resample
			B5=NIR	0.851-0.879	30*30
			TIR= B10,	10.60-11.19	100*(30)

#### IV. NORMALIZED DIFFERENCE VEGETATION INDEX (NDVI)

##### A. Calculation of Normalized Difference vegetation index (NDVI)

The Normalized difference vegetation index (NDVI) is calculated using the formula mention below (Chander and Markham, 2003). The NDVI value varies from -1 to 1.

Higher the value of it reflects high Near Infrared (NIR), means dense greenery (F. Zhang et al., 2016).

$$NDVI = ((NIR - Red)) / ((NIR + Red)) \quad (5)$$

where NIR is Band 4 for Landsat 5TM and Band 5 for Landsat 8 OLI and Red is Band 3 for Landsat 5TM and Band 4 for Landsat 8 OLI(Zhang et al., 2017).

#### V. RESULTS AND DISCUSSION

##### A. Spatiotemporal variations of NDVI in Varanasi City from 1992-2019

Table 2: Statistical Description (Minimum, Maximum, Mean and Standard Deviation) of NDVI for Pre-Monsoon Season in Varanasi City: 1992-2019

NDVI for Pre-Monsoon Season in Varanasi City: 1992-2019				
Year	Min	Max	Mean	Std dev.
1992	-0.0858	0.5799	0.2155	0.0913
2019	-0.0518	0.4862	0.134	0.0619

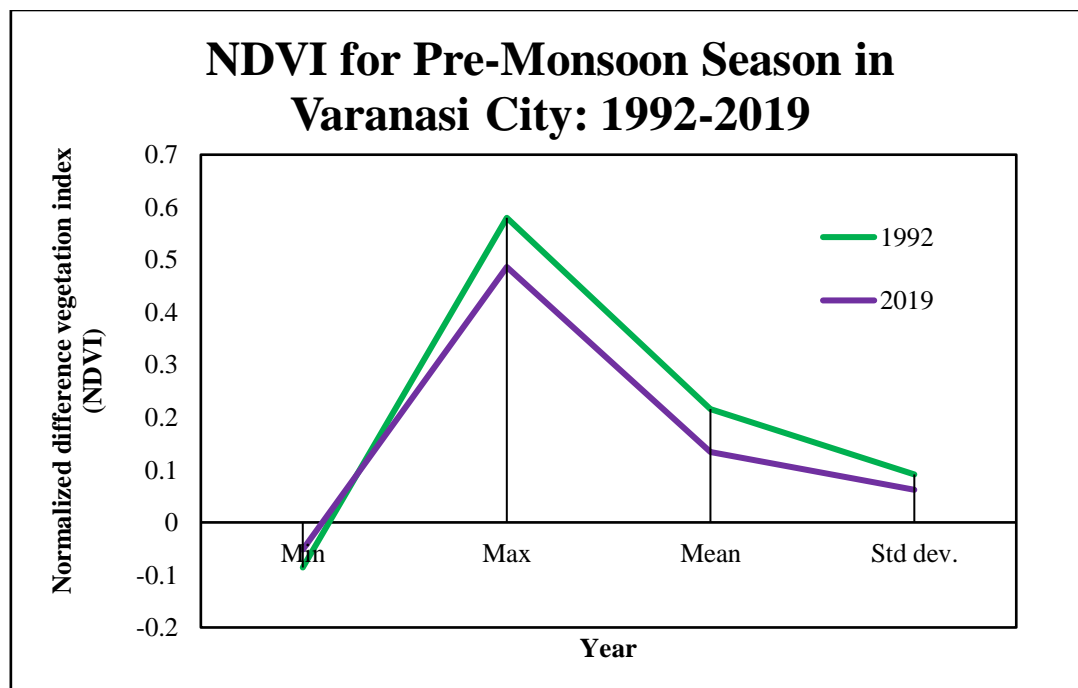


Fig. 2: Statistical Description (Minimum, Maximum, Mean and Standard Deviation) of NDVI for Pre-Monsoon Season in Varanasi City: 1992-2019

According to table 2, in 1992, the NDVI had a minimum value of -0.0858, a maximum value of 0.5799, a mean value of 0.2155, and a standard deviation of 0.0913. The 2019 NDVI values were as follows: -0.0518 for the minimum, 0.4862 for the highest, 0.134 for the mean, and 0.0619 for the standard deviation.

From this information, it is clear that the NDVI values in 1992 were generally lower than in 1992. This could be an indication of changes in vegetation cover or health in the area over time. However, it is difficult to draw conclusions without additional context such as the location and type of vegetation being measured.

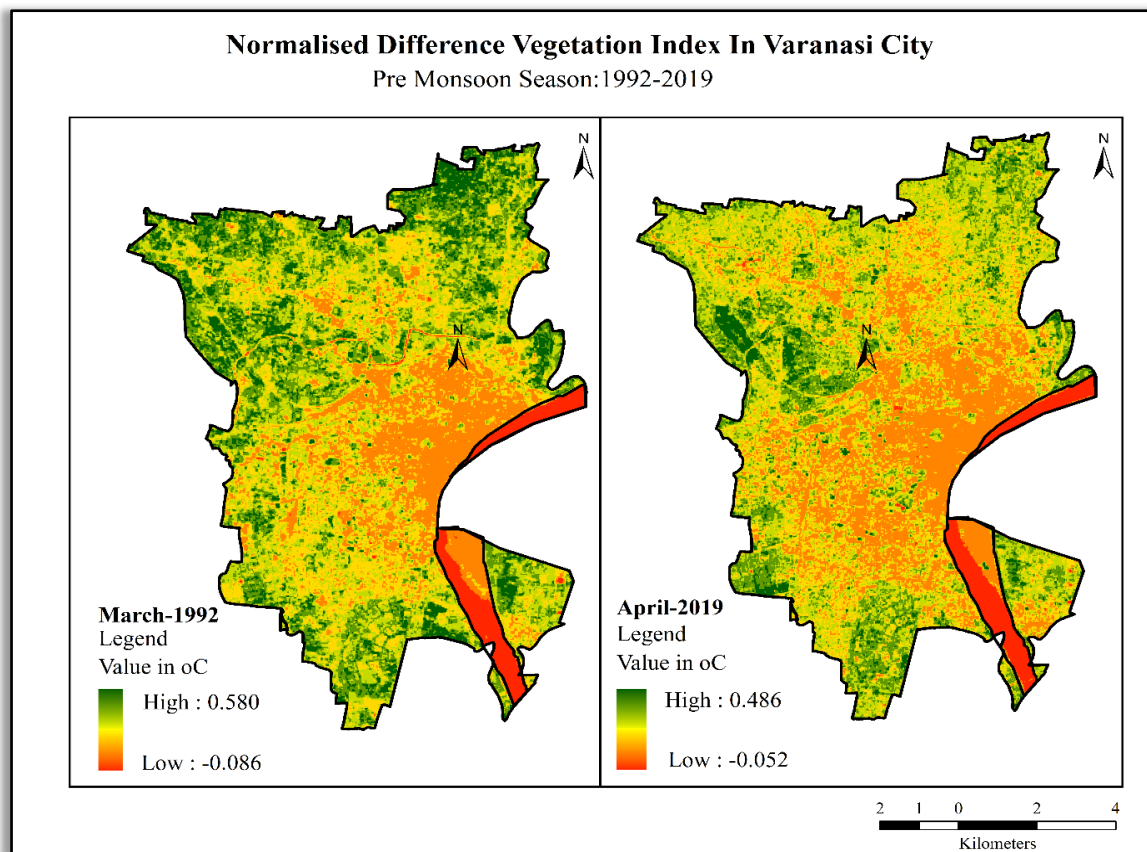


Fig. 3: Normalized Difference Vegetation Index (NDVI) (Left) and Enhanced Vegetation Index (EVI) (Right) for Pre-Monsoon Season in Varanasi City: 1992-2019

#### B. Spatiotemporal variations of NDVI for Pre-Monsoon Season in Varanasi City

The NDVI gauges the quantity and state of a region's vegetation at any particular time. Higher values for NDVI indicate denser or more scattered vegetation or built-up areas, respectively, whereas lower values indicate both. (Chakraborty, 2021; Shahfahad et al., 2020). The study's findings indicate that the Assi River, the vicinity of BHU, BLW, and the Cantonment area have the highest and most prominent NDVI, or vegetation greenness (Figure. 2). The NDVI was low in the majority of the city, and significant NDVI concentrations were only seen in sparsely populated areas. The north and centre of the area have the lowest NDVI values (Figure 3).

This table (Table 2.21) presents a statistical analysis of NDVI for the pre-monsoon season in Varanasi City during the years 1992 and 2019. The findings (Figure 3) revealed that the mean NDVI value declined from 0.2155 in 1992 to 0.1340 in 2019, indicating a decrease in vegetation density. NDVI values varied from -0.0858 to 0.5799.

## VI. CONCLUSION

In order to comprehend the dynamics of vegetation, the study analysed the spatiotemporal patterns of the Normalised Difference Vegetation Index (NDVI) in Varanasi, India. The results showed that the highest NDVI values, which indicate extensive vegetation, were found in the vicinity of the Assi River, BHU, BLW, and the Cantonment area. Low NDVI values were reported over most of the city, with high NDVI concentrations primarily occurring in sparsely populated areas. The mean NDVI value decreased from 0.2155 in 1992 to 0.1340 in 2019, according to a statistical analysis of NDVI data for the pre-monsoon season in Varanasi City between 1992 and 2019. These findings point to a possible decrease in vegetation cover, which might have severe effects on the ecosystem and people's health. Therefore, it is essential to keep an eye on Varanasi's vegetation dynamics and implement the necessary changes to preserve and improve the city's green spaces.



## ACKNOWLEDGEMENTS

The authors would like to thank Jamia Millia Islamia University for the support in research work and also acknowledge Varanasi Development authority (VDA), United States Geological Survey (USGS) and National Remote Sensing Centre (NRSC) for making remote sensing data accessible.

## REFERENCES

- [1.] Arnous, M. O. M., Basma M. H. (2022). Utilizing multi-temporal thermal data to assess environmental land degradation impacts: Example from Suez Canal region, Egypt. *Environmental Science and Pollution Research International*, 30(1), 2145–2163. <https://doi.org/10.1007/s11356-022-22237-z>
- [2.] Avdan, U., & Jovanovska, G. (2016). Algorithm for automated mapping of land surface temperature using LANDSAT 8 satellite data. *Journal of Sensors*, 2016. <https://doi.org/10.1155/2016/1480307>
- [3.] Babita Kumari, Mohammad Tayyab, Shahfahad, Salman, Javed Mallick, Mohd Firoz Khan, & Atiqur Rahman. (2018a). Satellite-Driven Land Surface Temperature (LST) Using Landsat 5, 7 (TM/ETM+ SLC) and Landsat 8 (OLI/TIRS) Data and Its Association with Built-Up and Green Cover Over Urban Delhi, India. *Remote Sensing in Earth Systems Sciences*, 1, 63–78. <https://doi.org/10.1007/s41976-018-0004-2>
- [4.] Babita Kumari, Mohammad Tayyab, Shahfahad, Salman, Javed Mallick, Mohd Firoz Khan, & Atiqur Rahman. (2018b). Satellite-Driven Land Surface Temperature (LST) Using Landsat 5, 7 (TM/ETM+ SLC) and Landsat 8 (OLI/TIRS) Data and Its Association with Built-Up and Green Cover Over Urban Delhi, India. *Remote Sensing in Earth Systems Sciences*, 1, 63–78. <https://doi.org/10.1007/s41976-018-0004-2>
- [5.] Bhanage, V. K., Sneha; Sharma, Rajat; Lee, Han; Gedam, Shirishkumar. (2023). Enumerating and Modelling the Seasonal alterations of Surface Urban Heat and Cool Island: A Case Study over Indian Cities. *Urban Science*, 7(2), 38. <https://doi.org/10.3390/urbansci7020038>
- [6.] Chakraborty, J. B., Deepalok; Dutta, Subrata B. (2021). A geospatial appraisal of urban expansion within the Teesta-Mahananda interfluvium in and around Siliguri town, West Bengal, India. In *Land Reclamation and Restoration Strategies for Sustainable Development* (Vol. 10, pp. 65–85). Elsevier. <https://doi.org/10.1016/b978-0-12-823895-0.00005-1>
- [7.] Cruz, J. A., Santos, J. A., & Blanco, A. (2020). SPATIAL DISAGGREGATION of LANDSAT-DERIVED LAND SURFACE TEMPERATURE over A HETEROGENEOUS URBAN LANDSCAPE USING PLANETSCOPE IMAGE DERIVATIVES. *International Archives of the Photogrammetry, Remote Sensing and Spatial Information Sciences - ISPRS Archives*, 43(B5), 115–122. <https://doi.org/10.5194/isprs-archives-XLIII-B5-2020-115-2020>
- [8.] Falguni Mukherjee. (2022). Environmental Impacts of Urban Sprawl in Surat, Gujarat: An Examination Using Landsat Data. *Journal of the Indian Society of Remote Sensing*, 50, 1003–1020. <https://doi.org/10.1007/s12524-022-01509-8>
- [9.] Glenn, E. P.; H., Alfredo; Nagler, Pamela L.; Hirschboeck, Katherine K.; Brown, Paul. (2007). Integrating Remote Sensing and Ground Methods to Estimate Evapotranspiration. *Critical Reviews in Plant Sciences*, 26(3), 139–168. <https://doi.org/10.1080/07352680701402503>
- [10.] Gutman, G. I., Alexander. (1998). The derivation of the green vegetation fraction from NOAA/AVHRR data for use in numerical weather prediction models. *International Journal of Remote Sensing*, 19(8), 1533–1543. <https://doi.org/10.1080/014311698215333>
- [11.] Huete, A. R. and J., R. D. and Post, D. F. (1985). Spectral response of a plant canopy with different soil backgrounds. *Remote Sensing of Environment*, 17, 37–53.
- [12.] Karthi, A.; A., S.; Sharma, Manish. (2022). Mapping of Compositional Diversity and Chronological Ages of Lunar Farside Multiring Mare Moscoviense Basin: Implications to the Middle Imbrian Mare Basalts. *Research in Astronomy and Astrophysics*, 22(12), 125002–125002. <https://doi.org/10.1088/1674-4527/ac8f8c>
- [13.] Kustas, W. P.; N., John M.; Anderson, Martha C.; French, Andrew N. (2003). Estimating subpixel surface temperatures and energy fluxes from the vegetation index-radiometric temperature relationship. *Remote Sensing of Environment*, 85(4), 429–440. [https://doi.org/10.1016/s0034-4257\(03\)00036-1](https://doi.org/10.1016/s0034-4257(03)00036-1)
- [14.] Mukherjee, F. (2022). Environmental Impacts of Urban Sprawl in Surat, Gujarat: An Examination Using Landsat Data. *Journal of the Indian Society of Remote Sensing*, 50(6), 1003–1020. <https://doi.org/10.1007/s12524-022-01509-8>
- [15.] Murari, V., Kumar, M., Mhawish, A., Barman, S. C., & Banerjee, T. (2017). Airborne particulate in Varanasi over middle Indo-Gangetic Plain: Variation in particulate types and meteorological influences. *Environmental Monitoring and Assessment*, 189(4), 157. <https://doi.org/10.1007/s10661-017-5859-9>
- [16.] Nidhi Singh, Alaa Mhawish, Santu Ghosh, Tirthankar Banerjee, & R.K. Mall. (2019). Attributing mortality from temperature extremes: A time series analysis in Varanasi, India. *Science of The Total Environment*, 665, 453–464. <https://doi.org/10.1016/j.scitotenv.2019.02.074>
- [17.] Ormsby, J. P. (1982). The use of Landsat-3 thermal data to help differentiate land covers. *Remote Sensing of Environment*, 12, 97–105.
- [18.] Ramankutty, N., & Foley, J. A. (1999). Estimating historical changes in global land cover: Croplands from 1700 to 1992. *Global Biogeochemical Cycles*, 13, 997–1027.

- [19.] Shahfahad, Kumari, B., Tayyab, M., Ahmed, I. A., Baig, M. R. I., Khan, M. F., & Rahman, A. (2020). Longitudinal study of land surface temperature (LST) using mono- and split-window algorithms and its relationship with NDVI and NDBI over selected metro cities of India. *Arabian Journal of Geosciences*, 13(19). <https://doi.org/10.1007/s12517-020-06068-1>
- [20.] Singh, N., Mhawish, A., Ghosh, S., Banerjee, T., & Mall, R. K. (2019). Attributing mortality from temperature extremes: A time series analysis in Varanasi, India. *Science of The Total Environment*, 665, 453–464. <https://doi.org/10.1016/j.scitotenv.2019.02.074>
- [21.] Verma, P., Singh, R., Bryant, C., & Raghubanshi, A. S. (2020). Green space indicators in a social-ecological system: A case study of Varanasi, India. *Sustainable Cities and Society*, 60. <https://doi.org/10.1016/j.scs.2020.102261>
- [22.] Weng, Q. (2009). Thermal infrared remote sensing for urban climate and environmental studies: Methods, applications, and trends. *ISPRS J. Photogramm. Remote Sens*, 64, 335–344.
- [23.] Wittich, K.-P. H., O. (1995). Area-averaged vegetative cover fraction estimated from satellite data. *International Journal of Biometeorology*, 38(4), 209–215. <https://doi.org/10.1007/bf01245391>
- [24.] Zhang, F., Tiyp, T., Kung, H., Johnson, V. C., Maimaitiyiming, M., Zhou, M., & Wang, J. (2016). Dynamics of land surface temperature (LST) in response to land use and land cover (LULC) changes in the Weigan and Kuqa river oasis, Xinjiang, China. *Arabian Journal of Geosciences*, 9(7). <https://doi.org/10.1007/s12517-016-2521-8>
- [25.] Zhang, X., Estoque, R. C., & Murayama, Y. (2017). An urban heat island study in Nanchang City, China based on land surface temperature and social-ecological variables. *Sustainable Cities and Society*, 32(May), 557–568. <https://doi.org/10.1016/j.scs.2017.05.005>